SIX DEGREES OF FREEDOM VIBRATION ISOLATION USING ELECTROMAGNETIC SUSPENSION

Sang-il Lee[1], Daniel B. DeBra[2], Peter F. Michelson[3],
Robert C. Taber[4], John C. Price[4]

ABSTRACT

Experimental data are presented for modelling an electromagnet. Control laws are considered with and without flux feedback and with position and orientation information of the suspended body. Base motion and sensor noise are the principal disturbances. Proper selection of the geometrical operating point minimizes the passive coupling above the bandwidth of the control and filtering can attenuate the high frequency content of sensor noise. Six electromagnets are arranged in a configuration which optimizes the load support and provides control over all six degrees of freedom of the suspended body. The design is based on experimental data generated with a specially designed test facility. Application for suspension of a gravity wave antenna is discussed.

INTRODUCTION

Isolation from base motion is frequently required. On the ground, precise instruments must be isolated from the cultural and natural seismic motion of the earth. In orbit, the motion of a spacecraft may be significant due to moving machinery, thrusters or the presence of man [1,2]. Many techniques are available. Mechanical devices such as coil springs, air cushions or compliant materials offer the advantage of simplicity and reliability. By using stacks of such devices, rapid attenuation with frequency can be achieved. But the mechanical link remains and when internal resonances, cross coupling of degrees of freedom and nonlinearity exist, the idealized attenuation hoped for is not always achieved. Passive or active feedback techniques using magnetic or electrostatic fields can remove the mechanical link and permit an improved degree of isolation. Examples include the electrostatic gyro [3] which can achieve spin down time constant of hundreds of years, passively suspended superconducting proof masses for a principle of equivalence experiment [4] and an eddy current suspension for gradiometers [5] and many forms of active and passive magnetic suspension reviewed by Jayawant [6]. An interesting variant is to shield a proof mass on orbit and use it as a reference thus producing a drag free satellite [7], which has achieved average disturbances of less than 5×10^{-12}g.

For an active isolation system, the suspended body follows its reference within the bandwidth of the feedback control. Thus isolation only occurs for frequencies above the bandwidth (natural frequency) of the control. Though the mechanical link is gone, displacement dependence of the force may remain and produces coupling which cannot be influenced by the feedback. Thus one desires to design an actuator which has no spatial dependence on force or has a local extremum so that the small-motion dependence is small. We will give an example later. The force used for suspension is generated as a function of measurements. These measurements are noisy and produce a component of force which is a disturbance. But the frequency content of this disturbance is under the control of the designer by appropriate filtering.

Certainly the most exquisitely sensitive instruments ever developed are the gravity wave antennas. Current bar antennas are capable of detecting strains of 10^{-18} and it is hoped bars can reach 10^{-20}

---

1. Graduate student, Dept. of Mechanical Engineering, Stanford University
2. Professor, Dept. of Aeronautics and Astronautics, Stanford University
3. Assistant Professor, Dept. of Physics, Stanford University
4. Research Associate, High Energy Physics Laboratory, Stanford University

with several improvements including better vibration isolation [8]. Optical measurements hold promise of reaching 10^{-22} strain [9]. The success with the existing bars has been achieved with an air cushion in combination with stacks of rubber and steel, producing an extremely sharp attenuation with frequency and an isolation in the frequency band from 500 to 1 kHz to levels below the Brownian noise in the bar. Vacuum and low temperature necessary for adequate isolation and sensitivity make the introduction of a large stack of isolators difficult, so an optimization has been performed to achieve the greatest isolation in a fixed volume [10].

For ultra-low temperature gravity wave antennas, it will be desirable to enclose the principal portions of the isolation system within the ultra-low (~ 100 mK) temperature region. If these structures are installed without adequate damping, nonlinear behavior can be expected. On the other hand, provision of an adequate degree of passive damping at these temperatures is challenging. Thus we have been looking at active means to provide magnetic suspension or quiet damping to an isolation stack. The results reported here are preliminary work on active magnetic suspension. We have followed an approach similar to the work of Rainer Weiss (Physic, MIT), where they are developing a 3 DOF active and 3 DOF passive suspension using Hall effect flux and optical fiber displacement feedback.

SYMBOLS

A	area
B	magnetic flux density
B_D	desired magnetic flux density
D	disturbance
f	frequency
F	force
F_D	desired force
$\Im$	magnetomotive force
g	gravitational acceleration
H	magnetic field intensity
i	current
i_D	desired current
l	length of the flux path in the solid
m	mass of the suspended body
N	number of turns
$\Re$	reluctance
$\Re_s$	reluctance due to solid magnetic circuit
s	Laplace transform variable
$S_i(f)$, $S_o(f)$	mean square spectral density
W	weight
z	air gap

z_D	desired air gap
z_g	ground motion
δ	error
ϕ	magnetic flux
μ_o	permeability of the air

THE ELECTROMAGNET

The force F between two parallel ferromagnetic surfaces with uniform magnetic flux density B between them is

$$F = - \frac{B^2 A}{2\mu_o} \tag{1}$$

where the minus sign signifies an attractive force, A is the area and μ_o is the permeability of the air (Figure 1). The magnetomotive force $\Im$ is due to permanent magnetism Hl and current in coils Ni. The flux ϕ and reluctance $\Re$ of the magnetic circuit which is dominated by the air gap then relate the flux density to current and gap

$$\Im = Hl + Ni \tag{2}$$

$$B = \frac{\phi}{A} = \frac{\Im}{\Re A} \tag{3}$$

$$\Re = \frac{z}{\mu_o A} + \Re_s \tag{4}$$

$$B = \frac{(Hl + Ni)\mu_o}{z(1 + \Re_s \mu_o A/z)} \tag{5}$$

To produce a desired control force F from (1), one must have a measure of B or use (2) with measures of the gap z and current i to produce B and thus F. The control is the current. An actual electromagnet has magnetic lines near the edge of its gap which are hard to calculate. Furthermore, the side force dependence on lateral deflection which we want to use for control is not easily calculated. So an electromagnet and two degrees of freedom test fixture was built to measure these quantities.

The experimental equipment shown in Figure 2 was designed to suspend a 10 pound mass. The set-up is mainly composed of two parts. The upper part is an electromagnet which has an annular cross section with core and can rotate about a vertical axis A-A offset from it. An annulus with a center core made of ferromagnetic material was chosen for the geometry of the electromagnet in order to minimize the loss and to provide the complete closed path of the magnetic flux. Magnetic flux density is measured by a Hall effect sensor located at the bottom of the center core in the upper housing which has a hole for the leads of the Hall effect sensor. The lower part is a cantilevered plate which can rotate about a horizontal axis B. At an equilibrium condition, the lower part

maintains a gap of 1 mm with respect to the upper part. The counterpart of the upper solenoid is made of the same ferromagnetic material, and the magnetic flux is supposed to pass through both of them. To reduce the dynamic range of the control current, a permanent magnet is used to provide the nominal flux and the control current provides only the small variations needed to maintain the average gap spacing. With two independent axes of rotation, vertical and horizontal motions can be measured by use of a displacement sensor when the magnetic flux density or the suspended mass is changed.

If the counterpart of the lower plate (Fig. 2) is flat and of uniform permeability, no lateral force develops with lateral displacement. By limiting the extent of the ferromagnetic material or introducing steps so that the geometry of the housing and counterpart match, more shearing of the field results. Static lateral force for the case of a step around the lower counterpart was investigated. Vertical interaction between the upper housing and the lower plate was eliminated by fixing the elevation of the lower plate. Figure 3 shows the experimental data of the relationship between the lateral force and the displacement as the current (and thus flux density) increases with 1 mm constant air gap. The lateral force increases until about 1.5 mm from the center, which corresponds to 60% of the thickness of the step and 150% of the gap and then decreases gradually. The slope of each curve at a certain point gives the lateral stiffness. If we wish to use two actuators to provide active control laterally each would be biased and a value of 0.75 mm would be of great interest. This combines passive stable performance and also active control. But for astatized pure feedback control, one might want to be at 1.5 mm. Figure 4 shows the experimental result on the vertical force according to the change in the vertical displacement. Fig. 3 and Fig. 4 are the data for passive behavior above the bandwidth of servos on both flux density and vertical displacement, which will be explained later.

VERTICAL MOTION CONTROL

As a consequence of Earnshaw's theorem [11], systems using permanent magnet or electromagnets (AC or DC) without the control of current are inherently unstable. In order, therefore, to achieve stable suspension it is necessary to devise a means of regulating the current in an electromagnet using position feedback, or others, of the object to be suspended. Two typical ways of stabilizing the system by use of an electromagnet are discussed by other researchers [12]. One is a pure feedback using only the gap information detected by a proximity sensor, and the other is a state feedback using the inertial information obtained by an accelerometer in addition to the gap information. As is stated earlier, one wants the supported element to be essentially attached to the foundation within the low frequency bandwidth of the feedback. Position feedback provides this link. Above the bandwidth of this control, one hopes to have complete isolation. A magnetic structure would have a constant force if the flux stayed constant. However, the reluctance changes as the gap changes and typically results a change in force. Thus one is motivated to remove this gap dependence above the bandwidth of the position feedback in order to reduce the coupling and linearize the outer loop. Flux feedback, which would keep the gap flux density constant, should do this. If a flux density transducer is introduced and used in conjunction with a feedback control loop to control the magnet current in such a manner that the gap flux density remains constant over the operating range of airgaps, the nonlinear force-displacement characteristics will be very linear. Figure 5 shows a block diagram with position and flux feedback for vertical motion control. Here PID control is used in the outer loop. An integrator is needed in the inner loop because there are no dynamics to reduce the magnitude of the feedback signal with frequency and therefore naturally cause a crossover which would limit the bandwidth. However, a sensor can only measure the flux density locally and even if spread throughout the gap, will miss the fringing flux. The flux density feedback should have a very wide bandwidth to reduce the gap dependent force to relatively high frequencies. The bandwidth reported by another study was 5 kHz [13]. In Figure 5, three possible noise sources are included. They are Hall effect sensor noise, displacement sensor noise and the ground motion as an external disturbance. The effects of these on the system response, especially on acceleration, are of great importance. Using the transfer function from each noise

source to the output acceleration, the effect of noise contents can be seen by the following equation if the frequency spectrum of the sensor noise is measured.

$$S_o(f) = |\text{Transfer Function}|^2 \, S_i(f) \qquad (6)$$

Here $S_i(f)$ and $S_o(f)$ are the input and output mean square spectral densities as functions of frequency.

CONTROL FOR SIX DEGREES OF FREEDOM

A configuration shown in Figure 6 and Figure 7 uses 3 sets of two electromagnets displaced from their centers in opposite directions. The geometrical operating point is the flat spot on the lateral force vs. displacement curve which for this electromagnet is 1.5 mm for a 1 mm gap. The lateral forces cancel when there is equal current but they do not when the current is unequal. The vertical force can be changed without disturbing the horizontal motion and by keeping the sum of the vertical forces constant the lateral force can be changed by increasing one while the other is reduced. When an electromagnet is displaced radially there is a radial force change. But the symmetry of the device insures there is no tangential force. Therefore the two horizontal directions for the suspended body have neutral passive stability for constant current and in principle there is no coupling above the bandwidth of the control for small amplitude vibrations of the ground.

The control of the six degrees of freedom can be accomplished with the six measurements shown in Fig. 6. Because the sensors are not at the center of the actuators one should use all six to provide precise information on the height and shear of each pair. But the sensor coupling is small and poses no threat to the stability of the system. The control coupling is about $1/\sqrt{3}$ and the sensor coupling can be made small by moving the sensor closer to the center point between each pair of actuators. Furthermore there is no resonant gain in the dynamics. The control can be calculated for each pair separately, estimating the force needed to restore the body to the correct gap and a centered lateral position. We are presently working on ways to reduce the slope of the vertical force with gap. A sketch in Figure 8 suggests a positive slope can be added to the vertical force dependence but at the expense of the horizontal slope. Earnshaw's theorem indicates a limit but we are currently studying actuator geometries that will provide the static forces for a given current needed for control as indicated above and at the same time minimize the slope of the force displacement curves for all degrees of freedom to minimize coupling above the control bandwidth.

CONCLUSIONS

Experimental data for force displacement relationship in the horizontal and vertical direction of an electromagnet were presented. Control laws were proposed with and without flux feedback in addition to position loop for the suspended body. Proper design of an electromagnet can give a passive zero stiffness operating region where the passive coupling above the bandwidth of the control can be minimized. The effect of base motion and sensor noise as principal disturbances to the vibration isolation must be minimized for example in the sense of minimizing the mean square spectral density of output acceleration. A control scheme for six degrees of freedom vibration isolation has been developed by use of the experimental model of an electromagnet and improved actuator characteristics are being developed to minimize high frequency passive coupling.

ACKNOWLEDGEMENT

This work is partially supported by the U.S. National Science Foundation under grants PHY85-13525 and PHY85-15856.

REFERENCES

1. N.Searby, "Effect of Science Laboratory Centrifuge on Space Station Environment," NASA/MSFC Workshop Proc. on "Measurement and characterization of the acceleration environment on board the space station," Guntersville, AL, Aug 1986

2. O.K.Garriott and D.B.DeBra, "A Simple Microgravity Table for the Orbiter or Space Station," Earth-Orient. Applic. Space Technol. Vol. 5, No. 3, 1985

3. R.A. Van Patten, "Flight Suspension for the Relativity Gyro," Marcel Grossman Conference, Sanghi, China, 1982

4. P.W.Worden, "Measurement of small forces with superconducting magnetic bearings," Precision Engineering Vol. 4, No. 3, July 1982

5. D.Sonnabend, "Mechanical Isolation for Gravity Gradiometers," NASA/MSFC Workshop Proc. on "Measurement and characterization of the acceleration environment on board the space station," Guntersville, AL, Aug 1986

6. B.V.Jayawant, "Electromagnetic suspension and levitation," IEE Proc., Vol. 129, Part A, No. 8, November 1982

7. Space Dept. of the Johns Hopkins University Applied Physics Lab. and Guidance & Control Lab. of Stanford University, "A Satellite Freed of all but Gravitational Forces: 'Triad I'," J. Spacecraft, Vol. 11, No. 9, Sept. 1974

8. P.F.Michelson, J.C.Price, R.C.Taber, "Resonant-Mass Detectors of Gravitational Radiation," Science, Vol. 237, 1987

9. A.D.Jeffries et al., "Gravitational Wave Observatories," Scientific American, Vol. 256, No. 6, June 1987

10. P.F.Michelson et al., "The Stanford Gravitational Wave Detection Program: A Plan for Observing the Next Supernova," The International Symposium on Experimental Gravitational Physics, Guang Zhou, PRC, 1987

11. S.Earnshaw, "On the nature of molecular forces which regulate the constitution of luminiferous ether," Trans. Camb. Phil. Soc., 1842, 7, pp. 97-112

12. J.K.Hedrick and D.N.Wormley, "Active suspensions for Ground Transport Vehicles - A State of the Art Review," Mechanics of Transportation Suspension Systems, The Winter Annual Meeting of ASME 1975

13. B.J.Hamilton, J.H.Andrus and D.R.Carter, "Pointing Mount with Active Vibration Isolation for Large Payloads," 10th annual AAS Guidance and Control Conference, 1987

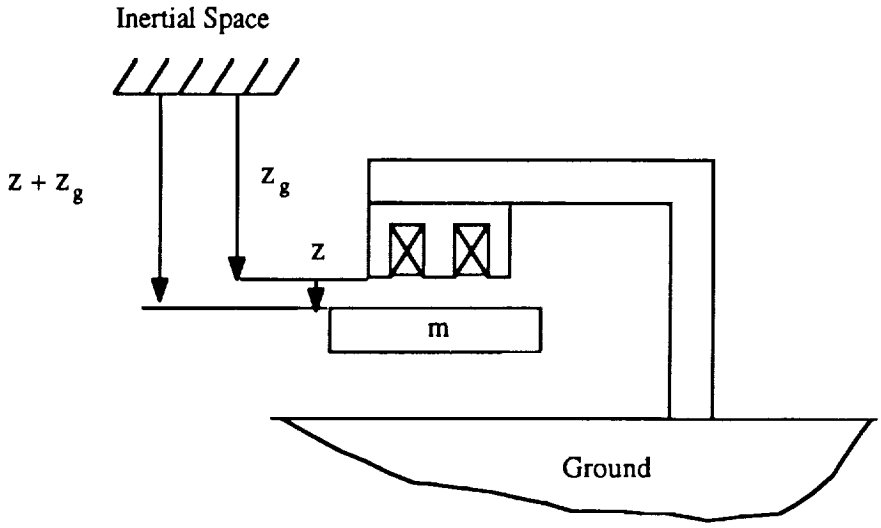

Figure 1 Coordinate System

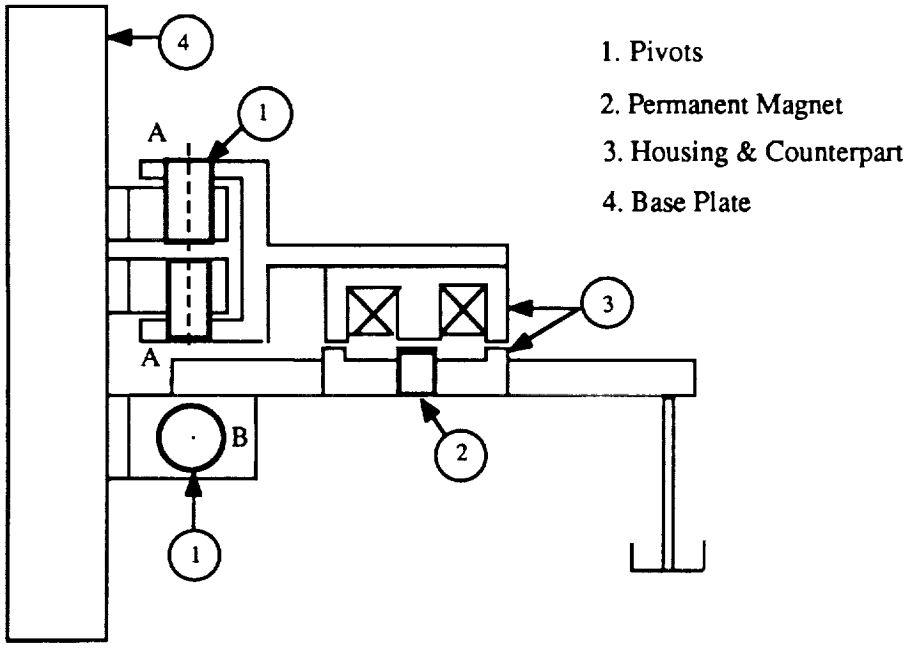

Figure 2 Schematic Diagram of Experimental Equipment

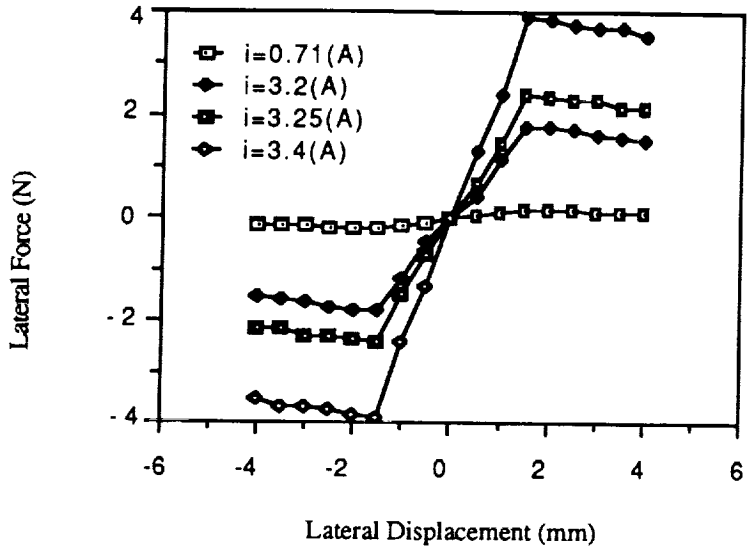

Figure 3 Lateral Force-Displacement Relation

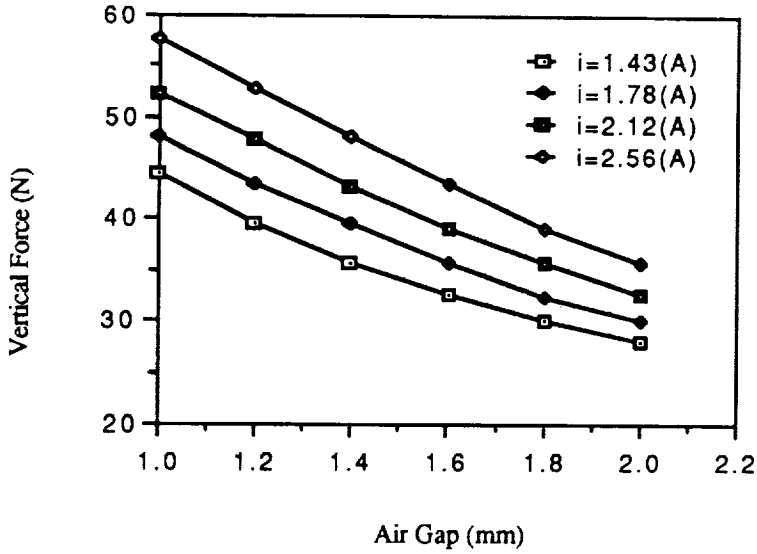

Figure 4 Vertical Force-Air Gap Relation

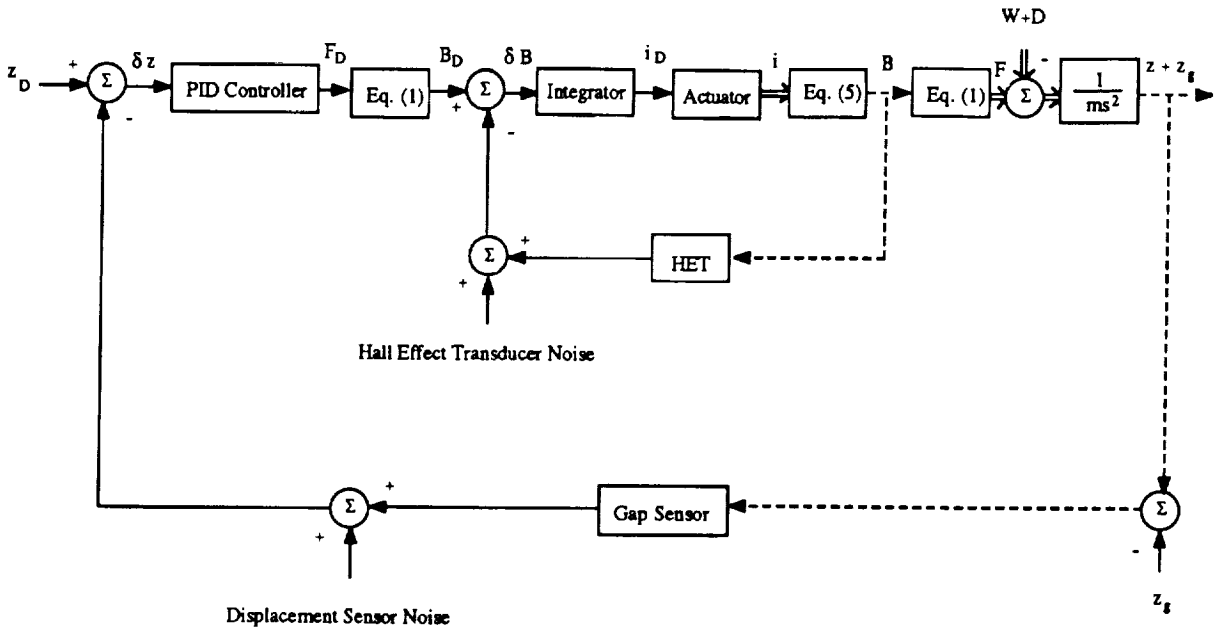

Figure 5 Block Diagram with Position and Flux Density Loop

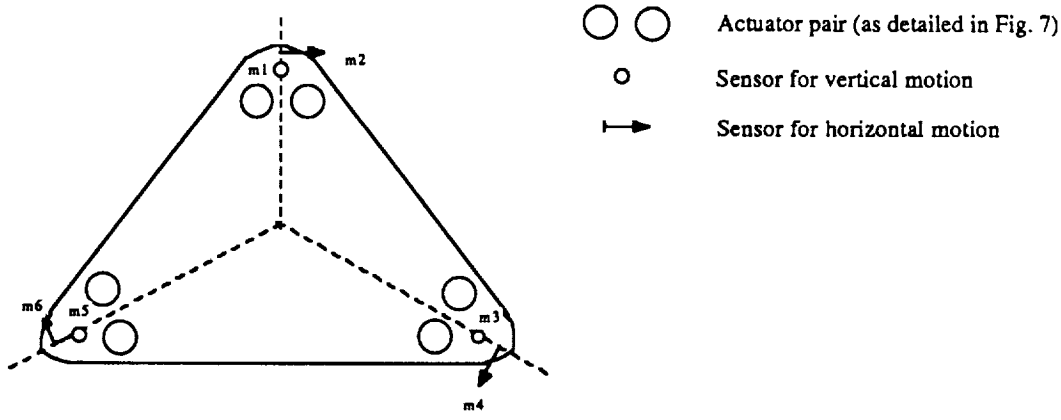

Figure 6 Configuration of Six Actuators and Sensors

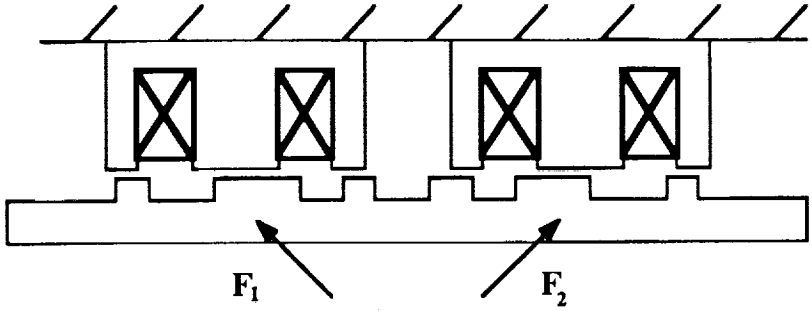

Figure 7 Two displaced electromagnets

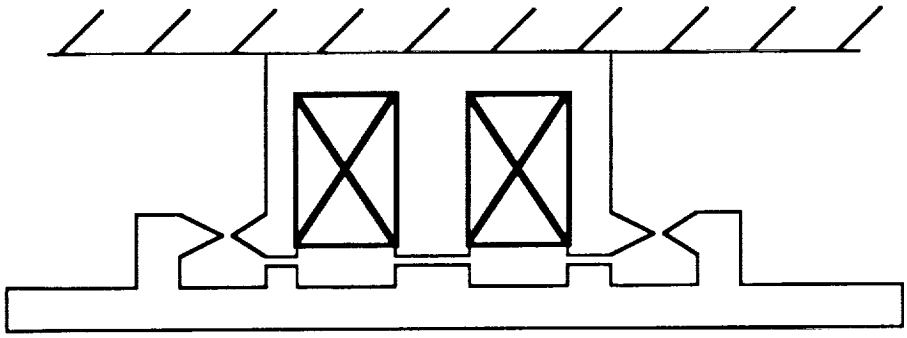

Figure 8 An actuator design with minor flux path with restoring force in vertical direction